

Thermal and non-thermal production of dark matter via Z' -portal(s)

Xiaoyong Chu^{a,*}, Yann Mambrini^{b,†}, Jérémie Quevillon^{b,‡} and Bryan Zaldivar^{c,§}

^a *Service de Physique Théorique Université Libre de Bruxelles, 1050 Brussels, Belgium*

^b *Laboratoire de Physique Théorique Université Paris-Sud, F-91405 Orsay, France*

^c *Instituto de Física Teórica, IFT-UAM/CSIC, 28049 Madrid, Spain*

We study the genesis of dark matter in the primordial Universe for representative classes of Z' -portals models. For weak-scale Z' mediators we compute the range of values of the kinetic mixing allowed by WMAP/PLANCK experiments corresponding to a FIMP regime. We show that very small values of δ ($10^{-12} \lesssim \delta \lesssim 10^{-11}$) are sufficient to produce the right amount of dark matter. We also analyse the case of very massive gauge mediators, whose mass $m_{Z'}$ is larger than the reheating temperature, T_{RH} , with a weak-scale coupling g_D to ordinary matter. Relic abundance constraints then impose a direct correlation between T_{RH} and the effective scale Λ of the interactions: $\Lambda \sim 10^3 - 10^5 \times T_{\text{RH}}$. Finally we describe in some detail the process of dark thermalisation and study its consequences on the computation of the relic abundance.

I. INTRODUCTION

Even if PLANCK [1] confirmed recently the presence of Dark Matter (DM) in the Universe with an unprecedented precision, its nature and its genesis are still unclear. The most popular scenario for the DM evolution is based on the mechanism of “thermal freeze-out” (FO) [2, 3]. In this scenario DM particles χ are initially in thermal equilibrium with respect to the thermal bath. When the temperature of the hot plasma T in the early Universe dropped below the DM mass, its population decreased exponentially until the annihilation rate into lighter species Γ_χ could not overcome the expansion rate of the Universe driven by the Hubble parameter $H(T)$. This defines the freeze-out temperature: $H(T_{\text{FO}}) \gtrsim \Gamma_\chi$. The comoving number density of the DM particles¹ and thus its relic abundance are then fixed to the value that PLANCK [1] and WMAP[4] observe today, $\Omega h^2 = 0.1199 \pm 0.0027$ at 68% CL. In this scenario it is obvious that the stronger the interaction between DM and the rest of the thermal bath is, the more DM pairs annihilate, ending-up with smaller relic densities. The detection prospects for frozen-out WIMPs are remarkable, since they involve cross-sections which can be probed nowadays with different experimental strategies, as production at colliders[5], Direct Detection (DD) and Indirect Detection (ID) experiments [6].

This popular freeze-out scenario is based on the hypothesis that the dark matter is initially produced at a democratic rate with the Standard Model (SM) particles. The so-called “WIMP miracle” can then be obtained if dark matter candidate has a mass of the electroweak scale and the dark sector and the Standard Model sector interact through electroweak strength coupling. Alternatively

one can relax the hypothesis of democratic production rate and suppose that the initial abundance of dark matter has been negligibly small whether by hierarchical or gravitational coupling to the inflaton or others mechanisms. This is the case for gravitino DM [7], Feebly Interacting Massive Particle dark matter (FIMP) in generic scenarios [8–10], scalar portals [11, 12], decaying dark matter [13] or Non Equilibrium Thermal Dark Matter (NETDM) [14].

Alternatively to the freeze-out, in the freeze-in (FI) mechanism the DM gets populated through interactions and decays from particles of the thermal bath with such an extremely weak rate (that is why called FIMP) that it never reaches thermal equilibrium with the plasma. In this case, the dark matter population n_χ grows very slowly until the temperature of the Universe drops below the mass m_χ . The production mechanism is then frozen by the expansion rate of the Universe $H(T_{\text{FI}})$. Contrary to the FO, in the FI scenario the stronger the interaction is, the larger the relic density results at the end, provided that the process never thermalises with the thermal bath. Due to the smallness of its coupling, the dark matter becomes very difficult to detect in colliders or direct detection experiments. However, one of the predictions of this scenario is that (visible) particles possibly decaying to dark matter need to have a long lifetime[8], so this peculiarity can be probed in principle in the LHC for example through the analysis of displaced vertices.

Very recently, it was analysed in [14] a scenario where the dark matter was also produced out-of-equilibrium, but differing from the orthodox FI mechanism in an essential way. In this new NETDM proposal the DM-SM couplings can be large (as for FO case), whereas the particle mediating the interaction is very heavy, which caused the evolution of dark matter number density to be dominated mostly by very high temperatures, just after the reheating epoch. This situation is opposite to the FI scenario where the couplings are feeble, typically $\mathcal{O}(10^{-11})$, and the portal is either massless or at least has a mass smaller than dark matter mass m_χ , causing the process to be dominated by low temperatures ($T \lesssim m_\chi$) instead.

In this work we study the dark matter candidate χ

* xiaoyong.chu@ulb.ac.be

† yann.mambrini@th.u-psud.fr

‡ jeremie.quevillon@th.u-psud.fr

§ b.zaldivar.m@csic.es

¹ Proportional to the yield $Y_\chi = n_\chi/s$, n_χ being the physical density of dark matter particles and s the entropy density.

populated by vector-like portals, whose masses lie in two different regimes: 1) A very heavy mediator, through the study of effective interactions of dark matter with the SM², and 2) An intermediate mediator, through the analysis of a kinetic-mixing model which contains a Z' acting as the portal. This study complements the case of massless vector-like mediators, studied in [10], showing distinct features concerning the evolution of the dark-sector independent thermalisation. On the other hand, we show the characteristics of the NETDM mechanism for a general vector-like interaction.

The paper is organised as follows. In section II a brief summary of non-thermalised production of dark matter particles is presented. Section III is devoted to present the two models of study, whose results are described in detail in section IV, before concluding in section V.

II. BOLTZMANN EQUATION AND PRODUCTION OF DARK MATTER OUT OF EQUILIBRIUM

If we consider that in the early stage of the Universe the abundance of dark matter has been negligibly small whether by inflation or some other mechanism, the solution of the Boltzmann equation can be solved numerically in effective cases like in [8] or in the case of the exchange of a massless hidden photon as did the authors of [10]. Such an alternative to the classical freeze out thermal scenario was in fact proposed earlier in [11] in the framework of the Higgs-portal model [12] and denominated “freeze in” [8]. If one considers a massive field Z' coupling to the dark matter, the dominant processes populating the DM particle χ are given by the decay $Z' \rightarrow \bar{\chi}\chi$ and the annihilation $\bar{S}M SM \rightarrow \bar{\chi}\chi$ involving the massive particle Z' as a mediator, or “portal” between the visible (SM) sector and the invisible (DM) sector. Our study will be as generic as possible by taking into account both processes at the same time, although we will show that for very large mediator masses $m_{Z'}$, or if the Z' is not part of the thermal bath, the decay process is highly suppressed, and the annihilation clearly dominates³. Under the Maxwell-Boltzmann approximation⁴ one can obtain an analytical solution of the DM yield adding the annihilation and decay processes:

$$\begin{aligned}
Y_\chi \approx & \left[\left(\frac{45}{\pi} \right)^{3/2} \frac{M_{\text{P}}}{4\pi^2} \right] \int_{T_0}^{T_{\text{RH}}} dT \int_{4m_\chi^2}^{\infty} ds \frac{1}{\sqrt{g_* g_*^s}} \frac{1}{T^5} \\
& \times K_1 \left(\frac{\sqrt{s}}{T} \right) \frac{1}{2048\pi^6} \sqrt{s - 4m_\chi^2} |\tilde{\mathcal{M}}_{2 \rightarrow 2}|^2 \\
& + \left[\left(\frac{45}{\pi} \right)^{3/2} \frac{M_{\text{P}}}{4\pi^2} \right] \int_{T_0}^{T_{\text{RH}}} dT \frac{1}{\sqrt{g_* g_*^s}} \frac{1}{T^5} \\
& \times K_1 \left(\frac{m_{Z'}}{T} \right) \frac{1}{128\pi^4} \sqrt{m_{Z'}^2 - 4m_\chi^2} |\tilde{\mathcal{M}}_{1 \rightarrow 2}|^2, \tag{1}
\end{aligned}$$

where M_{P} is the Planck mass, $T_0 = 2.7$ K the present temperature of the Universe, T_{RH} the reheating temperature, and K_1 is the 1st-order modified Bessel function of the second kind, g_* , g_*^s are the effective numbers of degrees of freedom of the thermal bath for the energy and entropy densities respectively. Finally, $|\tilde{\mathcal{M}}_{i \rightarrow 2}|^2 \equiv \int d\Omega |\mathcal{M}_{i \rightarrow 2}|^2$, where $\mathcal{M}_{i \rightarrow 2}$ is the squared amplitude of the process $i \rightarrow 2$ summed over all initial and final degrees of freedom, and Ω is the standard solid angle. Then, assuming a symmetric scenario for which the populations of χ and $\bar{\chi}$ are produced at the same rate, we can calculate the relic density

$$\Omega_\chi h^2 \approx \frac{m_\chi Y_\chi^0}{3.6 \times 10^{-9} \text{GeV}}, \tag{2}$$

where the super-index “0” refers to the value measured today. It turns out that the yield of the DM is actually sensitive to the temperature at which the DM is largely produced: at the beginning of the thermal history of the Universe if the mediator mass lies above the reheating temperature $m_{Z'} > T_{\text{RH}}$ (the so-called NETDM scenario [14]), or around the mass of the mediator if $2m_\chi < m_{Z'} < T_{\text{RH}}$ as the Universe plasma reaches the pole of the exchanged particle, in a resonance-like effect. Note that in the case of massless hidden photon or effective freeze-in cases described respectively in [10] and [8] the effective temperature scale defining the nowadays relic abundance is given by the only dark scale accessible, i.e. the mass of the DM (like in the classical freeze out scenario). In the following sections we will describe the two microscopic frameworks ($m_{Z'} > T_{\text{RH}}$ and $m_{Z'} < T_{\text{RH}}$) in which we have done our analysis.

III. THE MODELS

A. $m_{Z'} > T_{\text{RH}}$: effective vector-like interactions

If interactions between DM and SM particles involve very heavy particles with masses above the reheating temperature T_{RH} , we can describe them in the framework of effective field theory as a Fermi-like interaction can be a relatively accurate description of electroweak theories when energies involved in the interactions are below the

² Note that in this analysis, the nature of the mediator (vector or scalar) is not fundamental and our result can apply for the exchange of heavy scalars or heavy Higgses present in unified models also.

³ Note that in [8] the $2 \rightarrow 2$ annihilation process is considered subdominant with respect to the $1 \rightarrow 2$ decay process. However in the scenarios we will study, the annihilation dominates.

⁴ We have checked that the Maxwell-Boltzmann approximation induces a 10% error in the solution which justifies it to understand the general result. See [48] for an explicit cross-check of this approximation.

electroweak scale. Several works studying effective interactions in very different contexts have been done by the authors of [15]-[22] for accelerator constraints and [23]-[29] for some DM aspects. Depending on the nature of the DM we will consider the following effective operators, for complex scalar and Dirac fermionic DM ⁵:

Fermionic dark matter:

$$\mathcal{O}_V^f = \frac{1}{\Lambda_f^2} (\bar{f} \gamma^\mu f) (\bar{\chi} \gamma_\mu \chi), \quad (3)$$

leading to the squared-amplitude:

$$|\mathcal{M}_V^f|^2 = \frac{32N_c^f}{\Lambda_f^4} \left\{ \frac{s^2}{8} + 2 \left(\frac{s}{4} - m_f^2 \right) \left(\frac{s}{4} - m_\chi^2 \right) \cos^2 \theta + \frac{s}{2} (m_\chi^2 + m_f^2) \right\}. \quad (4)$$

Scalar dark matter:

$$\mathcal{O}_V^s = \frac{1}{\Lambda_f^2} (\bar{f} \gamma^\mu f) [(\partial_\mu \phi) \phi^* - \phi (\partial_\mu \phi)^*] \quad (5)$$

which leads to:

$$|\mathcal{M}_V^s|^2 = 4 \frac{N_c^f}{\Lambda_f^4} \left[-8 \left(\frac{s}{4} - m_f^2 \right) \left(\frac{s}{4} - m_\phi^2 \right) \cos^2 \theta + \left(\frac{s}{2} - m_f^2 \right) (s - 4m_\phi^2) + m_f^2 (s - 4m_\phi^2) \right]. \quad (6)$$

As we will show in section IV A, the main contribution to the population of DM in this case occurs around the reheating time. At this epoch, all SM particles f and the DM candidate χ can be considered as massless relativistic species.⁶ The expressions (4, 6) then become

$$\begin{aligned} |\mathcal{M}_V^f|^2 &\approx 4 \frac{N_c^f}{\Lambda_f^4} s^2 (1 + \cos^2 \theta), \\ |\mathcal{M}_V^s|^2 &\approx 2 \frac{N_c^f}{\Lambda_f^4} s^2 (1 - \cos^2 \theta), \end{aligned} \quad (7)$$

where, for simplicity and without loss of generality, we have considered universal effective scale $\Lambda_f \equiv \Lambda$. Considering different scales in the hadronic and leptonic sectors as was done in [17] for instance won't change appreciably our conclusions.

⁵ Other operators of the $\gamma_\mu \gamma^5$ pseudo-scalar types for instance can also appear for chiral fermionic DM, but we will neglect them as they bring similar contribution to the annihilation process.

⁶ This is justified numerically by the fact that large s ($\gtrsim 4T^2 \gg m_\chi^2(T), m_f^2(T)$) dominates the first integration in Eq.(1).

B. $m_{Z'} < T_{\text{RH}}$: extra Z' and kinetic mixing

1. Definition of the model

Neutral gauge sectors with an additional dark $U'(1)$ symmetry in addition to the SM hypercharge $U(1)_Y$ and an associated Z' are among the best motivated extensions of the SM, and give the possibility that a DM candidate lies within this new gauge sector of the theory. Extra gauge symmetries are predicted in most Grand Unified Theories (GUTs) and appear systematically in string constructions. Larger groups than $SU(5)$ or $SO(10)$ allow the SM gauge group and $U'(1)$ to be embedded into bigger GUT groups. Brane-world $U'(1)$ s are special compared to GUT $U'(1)$'s because there is no reason for the SM particles to be charged under them; for a review of the phenomenology of the extra $U'(1)$ s generated in such scenarios see e.g. [30]. In such framework, the extra Z' gauge boson would act as a portal between the “dark world” (particles not charged under the SM gauge group) and the “visible” sector.

Several papers considered that the “key” of the portal could be the gauge invariant kinetic mixing $(\delta/2) F_Y^{\mu\nu} F'_{\mu\nu}$ [31, 32]. One of the first models of DM from the hidden sector with a massive additional $U'(1)$, mixing with the SM hypercharge through both mass and kinetic mixings, can be found in [33]. The DM candidate χ could be the lightest (and thus stable) particle of this secluded sector. Such a mixing has been justified in recent string constructions [34–38], supersymmetry [39], $SO(10)$ framework [40] but has also been studied within a model independent approach [41–43] with vectorial dark matter [44] or extended extra- $U(1)$ sector [45]. For typical smoking gun signals in such models, like a monochromatic gamma-ray line, see [46].

The matter content of any dark $U'(1)$ extension of the SM can be decomposed into three families of particles:

- The *Visible sector* is made of particles which are charged under the SM gauge group $SU(3) \times SU(2) \times U_Y(1)$ but not charged under $U'(1)$ (hence the “dark” denomination for this gauge group).
- The *Dark sector* is composed of the particles charged under $U'(1)$ but neutral with respect to the SM gauge symmetries. The DM (χ) candidate is the lightest particle of the dark sector.
- The *Hybrid sector* contains states with SM and $U'(1)$ quantum numbers. These states are fundamental because they act as a portal between the two previous sectors through the kinetic mixing they induce at loop order.

From these considerations, it is easy to build the effective

Lagrangian generated at one loop :

$$\begin{aligned} \mathcal{L} = & \mathcal{L}_{\text{SM}} - \frac{1}{4} \tilde{B}_{\mu\nu} \tilde{B}^{\mu\nu} - \frac{1}{4} \tilde{X}_{\mu\nu} \tilde{X}^{\mu\nu} - \frac{\delta}{2} \tilde{B}_{\mu\nu} \tilde{X}^{\mu\nu} \\ & + i \sum_i \bar{\psi}_i \gamma^\mu D_\mu \psi_i + i \sum_j \bar{\Psi}_j \gamma^\mu D_\mu \Psi_j, \end{aligned} \quad (8)$$

\tilde{B}_μ being the gauge field for the hypercharge, \tilde{X}_μ the gauge field of $U'(1)$ and ψ_i the particles from the hidden sector, Ψ_j the particles from the hybrid sector, $D_\mu = \partial_\mu - i(q_Y \tilde{g}_Y \tilde{B}_\mu + q_D \tilde{g}_D \tilde{X}_\mu + g T^a W_\mu^a)$, T^a being the $SU(2)$ generators, and

$$\delta = \frac{\tilde{g}_Y \tilde{g}_D}{16\pi^2} \sum_j q_Y^j q_D^j \log \left(\frac{m_j^2}{M_j^2} \right) \quad (9)$$

with m_j and M_j being hybrid mass states [47]. It has been showed [32] that the value of δ may be as low as 10^{-14} , e.g. in the case of gauge-mediated SUSY-breaking models, where the typical relative mass splitting $|M_j - m_j|/M_j$ is extremely small.

Notice that the sum is on all the hybrid states, as they are the only ones which can contribute to the \tilde{B}_μ , \tilde{X}_μ propagator. After diagonalising of the current eigenstates that makes the gauge kinetic terms of Eq.(8) diagonal and canonical, we can write after the $SU(2)_L \times U(1)_Y$ breaking⁷

$$\begin{aligned} A_\mu &= \sin \theta_W W_\mu^3 + \cos \theta_W B_\mu \\ Z_\mu &= \cos \phi (\cos \theta_W W_\mu^3 - \sin \theta_W B_\mu) - \sin \phi X_\mu \\ Z'_\mu &= \sin \phi (\cos \theta_W W_\mu^3 - \sin \theta_W B_\mu) + \cos \phi X_\mu \end{aligned} \quad (10)$$

with, to first order in δ ,

$$\begin{aligned} \cos \phi &= \frac{\alpha}{\sqrt{\alpha^2 + 4\delta^2 \sin^2 \theta_W}} \quad \sin \phi = \frac{2\delta \sin \theta_W}{\sqrt{\alpha^2 + 4\delta^2 \sin^2 \theta_W}} \\ \alpha &= 1 - m_{Z'}^2/M_Z^2 - \delta^2 \sin^2 \theta_W \\ &\pm \sqrt{(1 - m_{Z'}^2/M_Z^2 - \delta^2 \sin^2 \theta_W)^2 + 4\delta^2 \sin^2 \theta_W} \end{aligned} \quad (11)$$

and $+$ ($-$) sign if $m_{Z'} < (>)M_Z$. The kinetic mixing parameter δ generates an effective coupling of SM states ψ_{SM} to Z' , and a coupling of χ to the SM Z boson which induces an interaction on nucleons. Developing the covariant derivative on SM and χ fermions state, we computed the effective $\psi_{\text{SM}} \psi_{\text{SM}} Z'$ and $\chi \chi Z$ couplings to first order⁸ in δ and obtained

$$\mathcal{L} = q_D \tilde{g}_D (\cos \phi Z'_\mu \bar{\chi} \gamma^\mu \chi + \sin \phi Z_\mu \bar{\chi} \gamma^\mu \chi). \quad (12)$$

In the rest of the analysis, we will use the notation $\tilde{g}_D \rightarrow g_D$. We took $q_D g_D = 1$ through our analysis, keeping in mind that for the $m_{Z'}$ -regimes we consider here, our results stay completely general by a simple rescaling of the kinetic mixing δ if the dominant process transferring energy from SM to DM is $\bar{f}f \rightarrow Z'^{(*)} \rightarrow \bar{\chi}\chi$; whereas if processes involving on-shell Z' dominate, the results become nearly independent of $q_D g_D$.

2. Processes of interest

As is clear from the model defined above, both DM and SM particles will interact via the standard Z or the extra Z' boson. Thus a priori there are four processes contributing to the DM relic abundance: $\bar{f}f \rightarrow V \rightarrow \bar{\chi}\chi$, and $V \rightarrow \bar{\chi}\chi$, where V can be Z and/or Z' , and in the $2 \rightarrow 2$ process both Z and Z' interfere to produce the total cross-section.⁹ The amplitudes of those processes are:

$$|\mathcal{M}_{2 \rightarrow 2}|^2 = |\mathcal{M}_Z|^2 + |\mathcal{M}_{Z'}|^2 + (\mathcal{M}_Z \mathcal{M}_{Z'}^* + \text{h.c.}), \quad (13)$$

where

$$\begin{aligned} |\mathcal{M}_Z|^2 &= \frac{(q_D g_D)^2 \sin^2 \phi}{(s - M_Z^2)^2 + (M_Z \Gamma_Z)^2} \\ &\times \{ (c_L^2 + c_R^2) [16m_\chi^2 m_f^2 (\cos^2 \theta - \sin^2 \theta) \\ &+ 8m_\chi^2 s \sin^2 \theta - 8m_f^2 s \cos^2 \theta + 2s^2 (1 + \cos^2 \theta)] \\ &+ c_L c_R (32m_\chi^2 m_f^2 + 16m_f^2 s) \}, \end{aligned} \quad (14)$$

$$\begin{aligned} |\mathcal{M}_{Z'}|^2 &= |\mathcal{M}_Z|^2 \quad \text{with : } [\sin \phi \rightarrow \cos \phi, \\ (M_Z, \Gamma_Z) &\rightarrow (m_{Z'}, \Gamma_{Z'}), \quad (c_L, c_R) \rightarrow (c'_L, c'_R)], \end{aligned} \quad (15)$$

and

$$\begin{aligned} \mathcal{M}_Z \mathcal{M}_{Z'}^* + \text{h.c.} &= \frac{2A (q_D g_D)^2 \sin \phi \cos \phi}{A^2 + B^2} \\ &\times \{ (c_L c'_L + c_R c'_R) [16m_\chi^2 m_f^2 (\cos^2 \theta - \sin^2 \theta) \\ &+ 8m_\chi^2 s \sin^2 \theta - 8m_f^2 s \cos^2 \theta + 2s^2 (1 + \cos^2 \theta)] \\ &+ (c_L c'_R + c_R c'_L) (16m_\chi^2 m_f^2 + 8m_f^2 s) \}, \end{aligned} \quad (16)$$

with

$$\begin{aligned} A &= s^2 - s(M_Z^2 + m_{Z'}^2) + M_Z^2 m_{Z'}^2 + M_Z m_{Z'} \Gamma_Z \Gamma_{Z'} \\ B &= s(\Gamma_Z M_Z - \Gamma_{Z'} m_{Z'}) + M_Z^2 m_{Z'} \Gamma_{Z'} - m_{Z'}^2 M_Z \Gamma_Z, \end{aligned} \quad (17)$$

⁷ Our notation for the gauge fields are $(\tilde{B}^\mu, \tilde{X}^\mu)$ before the diagonalization, (B^μ, X^μ) after diagonalization and (Z^μ, Z'^μ) after the electroweak breaking.

⁸ One can find a detailed analysis of the spectrum and couplings of the model in the appendix of Ref.[43]. The coupling g_D is the effective dark coupling \tilde{g}_D after diagonalization.

⁹ There are additional processes, not written here, which can have non-negligible influence on the final DM number density; e.g. $\bar{f}f \rightarrow ZZ' \rightarrow Z\bar{\chi}\chi$, with a t -channel exchange of a fermion f . These processes have been taken into account in the full numerical solution of the coupled set of Boltzmann equations, as shown below.

whereas for the $1 \rightarrow 2$ process we have:

$$|\mathcal{M}_{1 \rightarrow 2}|^2 = \begin{cases} 4(q_D g_D)^2 (\sin^2 \phi) (M_Z^2 + 2m_\chi^2) & \text{if } V = Z \\ 4(q_D g_D)^2 (\cos^2 \phi) (m_{Z'}^2 + 2m_\chi^2) & \text{if } V = Z' \end{cases} \quad (18)$$

Here the coefficients $c_{L,R}$ and $c'_{L,R}$ are the left and right couplings of the SM fermions to the Z and Z' bosons, respectively. Their explicit forms are shown in the appendix.

IV. RESULTS AND DISCUSSION

A. $m_{Z'} > T_{RH}$

In the case of production of DM through SM particle annihilation, the Boltzmann equation can be simplified

$$\frac{dY}{dx} = \frac{1}{16(2\pi)^8} \frac{1}{g_* \sqrt{g_*^s}} \left(\frac{45}{\pi}\right)^{3/2} \frac{M_p}{m_\chi} \quad (19)$$

$$\times \int_{2x}^{\infty} z (z^2 - 4x^2)^{1/2} K_1(z) dz |\mathcal{M}(z)|^2 d\Omega$$

with $z = \sqrt{s}/T$, $x = m_\chi/T$ and Ω the solid angle of the outgoing DM particles. Using the expression for $|\mathcal{M}|^2$ obtained in Eq.(7) we can write an analytical expression of the relic yields present nowadays if we suppose (as we will check) that the non-thermal production of DM happens at temperatures (and thus s) much larger than the mass of DM or SM particles ($m_f, m_\chi \ll \sqrt{s}$). After integrating over the temperature (x to be precise) from T_{RH} to T , and considering that all the fermions of the SM contribute democratically ($\Lambda_f \equiv \Lambda$) one obtains¹⁰

$$Y_V^f(T) \simeq \frac{4}{3} \frac{384}{(2\pi)^7} \left(\frac{45}{\pi g_*^s}\right)^{3/2} \frac{M_p}{\Lambda^4} \left[T_{RH}^3 - T^3\right],$$

$$Y_V^s(T) \simeq \frac{1}{3} \frac{384}{(2\pi)^7} \left(\frac{45}{\pi g_*^s}\right)^{3/2} \frac{M_p}{\Lambda^4} \left[T_{RH}^3 - T^3\right], \quad (20)$$

where $g_* \sim g_*^s$ has been used. We show in Fig. (1) the evolution of $Y(T)$ for a fermionic DM as a function of $x = m_\chi/T$ with $m_\chi = 100$ GeV for two different reheating temperatures, $T_{RH} = 10^8$ and 10^9 GeV. We note that to obtain analytical solution to the Boltzmann equation, we approximated the Fermi-Dirac/Bose-Einstein by Maxwell-Boltzmann distribution. This can introduce a 10% difference with respect to the exact case [48]. However, when performing our study we obviously solved numerically the complete set of Boltzmann equations. As

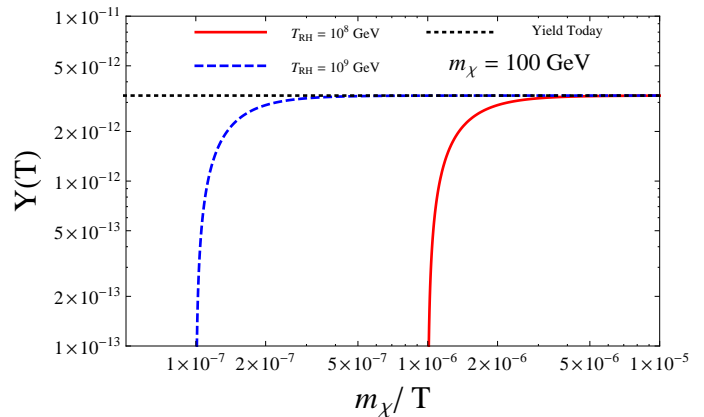


FIG. 1. Evolution of the number density per comoving frame ($Y = n/s$) for a 100 GeV fermionic DM as a function of m_χ/T for two reheating temperatures, $T_{RH} = 10^8$ (red) and 10^9 (blue) GeV in the case of vector interaction for fermionic a DM candidate. The value of the scale Λ has been chosen such that the nowadays yield Y corresponds to the nowadays value of $Y(T_0)$ measured by WMAP: $Y(T_0) \simeq 3.3 \times 10^{-12}$ represented by the horizontal black dashed line (see the text for details).

one can observe in Fig. (1), the relic abundance of the DM is saturated very early in the Universe history, around $T \simeq T_{RH}$, confirming our hypothesis that we can consider all the particles in the thermal bath (as well as the DM) as massless in the annihilation process: $m_\chi, m_f \ll \sqrt{s}$. At $T \simeq T_{RH}/2$ the DM already reaches its asymptotical value.

Moreover, for a given value of the reheating temperature T_{RH} , we compute the effective scale Λ such that the present DM yield $Y(T_0)$ respects the value measured by WMAP/PLANCK: $Y(T_0) \simeq 3.3 \times 10^{-12}$ for a 100 GeV DM. Imposing this constraint in Eq.(20), we obtain $\Lambda(T_{RH} = 10^8 \text{ GeV}) \simeq 3.9 \times 10^{12}$ GeV and $\Lambda(T_{RH} = 10^9 \text{ GeV}) \simeq 2.2 \times 10^{13}$ GeV for a fermionic DM.

As a consequence, we can derive the value of Λ respecting the WMAP/PLANCK constraint as a function of the reheating temperature T_{RH} for different masses of DM. This is illustrated in Fig. (2) where we solved numerically the exact Boltzmann equation. We observe that the values of Λ we obtained with our analytical solutions -extracted from Eqs.(20)- are pretty accurate and the dependence on the nature (fermion or scalar) of the DM is very weak. We also notice that the effective scale needed to respect WMAP constraint is very consistent with GUT-like SO(10) models which predict typical 10^{12-14} GeV as intermediate scale if one imposes unification [14]. Another interesting point is that $\Lambda \gg T_{RH}$ whatever is the nature of DM, ensuring the coherence of the effective approach. We have also plotted the result for very heavy DM candidates (PeV scale) to show that in such a scenario, there is no need for the DM mass to lie within electroweak limits, avoiding any “mass fine tuning” as in the classical WIMP paradigm.

We also want to underline the main difference with an

¹⁰ Notice that the factor of difference corresponds to the different degrees of freedom for a real scalar and Dirac fermionic DM.

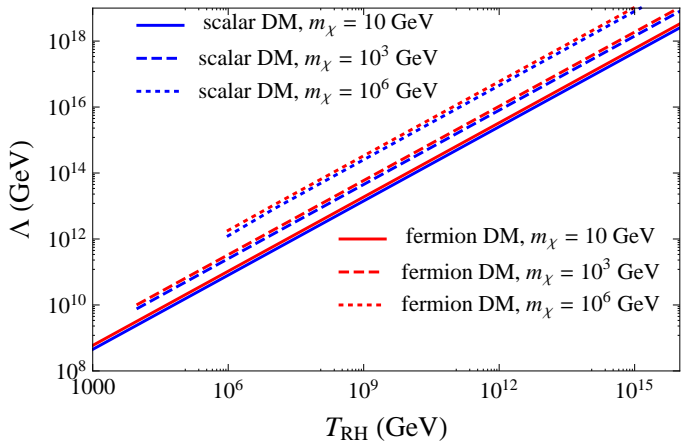


FIG. 2. Values of the scale Λ for fermionic (red) and scalar (blue) DM, assuming good relic abundance ($\Omega_\chi h^2 = 0.12$) and DM mass of 10 GeV (solid), 1000 GeV (dashed) and 10⁶ GeV (dotted), as a function of the reheating temperature.

infrared-dominated “freeze in” scenario, where the DM is also absent in the early Universe. Indeed, in orthodox freeze-in, the relic abundance increases very slowly as a function of m_χ/T , and the process which populates the Universe with DM is frozen at the time when the temperature drops below the mass of the dark matter, Boltzmann-suppressing its production by the thermal bath, which does not have sufficient energy to create it through annihilation. This can be considered as a fine tuning: the relic abundance should reach the WMAP value at a definite time, $T \simeq m_\chi/3$. In a sense, it is a common feature among freeze-in and freeze-out scenarios. In both cases the fundamental energy scale which stops the (de)population process is m_χ/T . When the mediator mass $m_{Z'}$ is larger than the reheating temperature, the fundamental scale which determines the relic abundance is $T_{\text{RH}}/m_{Z'}$ or T_{RH}/Λ in the effective approach. The DM abundance is then saturated from the beginning, at the reheating time, and thus stays constant during the rest of the thermal history of the Universe, and is nearly independent of the mass of the DM: no fine tuning is required, and no “special” freeze-in at $T \simeq m_\chi/3$. This is a particular case of the NETDM framework presented in [14]. Furthermore, the NETDM mechanism has the interesting properties to avoid large thermal corrections to dark matter mass. The reason is that all dark sector particles are approximately decoupled from the visible medium of the Universe.¹¹

¹¹ While the thermal masses of visible particles may change the DM production rate, we have checked that this effect is negligible.

B. $m_{Z'} < T_{\text{RH}}$

1. Generalities

The case of light mediators (in comparison to the reheating temperature) is more complex and rises several specific issues. We concentrate in this section on the computation of the DM relic abundance in the kinetic-mixing framework because it can be easily embedded in several ultraviolet completions. However, our analysis is valid for any kind of models with an extra $U(1)$ gauge group. The kinetic mixing δ is indeed completely equivalent to an extra $U(1)$ millicharge for the visible sector and one can think δ as the charge of the SM particles (visible world) to the Z' . Cosmological constraints allow us to restrict the parameter space of the model in the plane $(\delta, m_{Z'}, m_\chi)$. However we should consider two options for the mediator Z' : either it is in thermal equilibrium with the SM plasma, or, in analogy with the DM, it has not been appreciably produced during the reheating phase. The differential equation for the decay process $Z' \rightarrow \bar{\chi}\chi$, in the case where the DM annihilation is neglected, can be expressed as:

$$\frac{dY}{dx} = \frac{m_{Z'}^3 \Gamma_{Z'} g_{Z'}}{2\pi^2 H x^2 s} K_1(x). \quad (21)$$

where $x \equiv m_{Z'}/T$, $\Gamma_{Z'}$ the decay width of Z' and $g_{Z'} = 3$ giving the degree of freedom of the massive gauge boson Z' . Expressing the entropy and Hubble parameter as:

$$s = g_*^s \frac{2\pi^2}{45} \frac{m_{Z'}^3}{x^3}, \quad H = \sqrt{g_*} \sqrt{\frac{4\pi^3}{45}} \frac{m_{Z'}}{x^2 M_p}$$

we finally obtain the equation

$$Y_0 \approx \left(\frac{45}{\pi}\right)^{\frac{3}{2}} \frac{1}{g_*^s \sqrt{g_*}} \frac{M_p \Gamma_{Z'} g_{Z'}}{8\pi^4 m_{Z'}^2} \int_{\frac{m_{Z'}}{T_{\text{RH}}}}^{\infty} x^3 K_1(x) dx. \quad (22)$$

Approximating $\Gamma_{Z'} \simeq q_D^2 g_D^2 m_{Z'}/(16\pi)$, $q_D g_D$ being the effective gauge coupling of Z' and DM, and also taking $g_*^s \simeq g_*$ at the energies of interest, we can write

$$Y_0 \simeq \left(\frac{45}{\pi}\right)^{3/2} \frac{q_D^2 g_D^2 M_p}{128\pi^5 m_{Z'}} \int_{\frac{m_{Z'}}{T_{\text{RH}}}}^{\infty} x^3 K_1(x) dx. \quad (23)$$

Using $\int_0^\infty x^3 K_1(x) dx \simeq 4.7$ and Eq.(2) we obtain

$$\Omega_0 h^2 \simeq 2 \times 10^{22} q_D^2 g_D^2 \frac{m_\chi}{m_{Z'}}. \quad (24)$$

To respect WMAP/Planck data in a FIMP scenario one thus needs $g_D \simeq 10^{-11}$ if Z' is at TeV scale. For much higher values of g_D , the DM joins the thermal equilibrium at a temperature $T \gg m_\chi$ and then recovers the classical freeze out scenario.

Thus, a first important conclusion is that a Z' in thermal equilibrium with the plasma and decaying dominantly to

DM would naturally overpopulate the DM which would thus thermalise with plasma, ending up with the standard freeze-out history. We then have no choice than to concentrate on the alternative scenario where Z' , same as the DM, was not present after inflation. Thus the interaction of the SM bath (and the DM generated from it) could create it in a considerable amount. This is discussed below.

2. Chemical equilibrium of the dark sector

If Z' is generated largely enough at some point during the DM genesis, it will surely affect the DM final relic abundance through the efficient DM- Z' interactions. In the study of the evolution of the Z' population it may happen that Z' enters in a state of chemical equilibrium exclusively with DM, independently of the thermal SM bath, and thus with a different temperature. This “dark thermalisation” can have some effect on the final DM number density. The analysis we perform here is inspired from [10], which was however applied to a different model.

If the Z' -DM scattering rate is larger than the Hubble expansion rate of the Universe¹², these two species naturally reach kinetic equilibrium, with a well defined temperature T' , which a priori is different from (and is a function of) the thermal bath (photon) temperature, T . This temperature T' increases slowly (given the feeble couplings) due to the transfer of energy from the thermal bath, which determines the energy density ρ' and pressure P' of the dark sector. The Boltzmann equation governing the energy transfer in this case is:

$$\begin{aligned} \frac{d\rho'}{dt} + 3H(\rho' + P') &= \int \prod_{i=1}^4 d^3\bar{p}_i f_1(p_1) f_2(p_2) \\ &\times |\mathcal{M}|^2 (2\pi)^4 \delta^{(4)}(p_{\text{in}} - p_{\text{out}}) \cdot E_{\text{trans.}} \\ &= \frac{1}{2048\pi^6} \int_{4m_\chi^2}^{\infty} ds K_2\left(\frac{\sqrt{s}}{T}\right) T \sqrt{(s - 4m_\chi^2)s} |\tilde{\mathcal{M}}_{12 \rightarrow \chi\bar{\chi}}|^2 \\ &+ \frac{1}{128\pi^4} K_2\left(\frac{m_{Z'}}{T}\right) m_{Z'} T \sqrt{m_{Z'}^2 - 4m_1^2} |\tilde{\mathcal{M}}_{Z' \rightarrow 12}|^2, \quad (25) \end{aligned}$$

where 1 and 2 are the initial SM particles and $m_1 = m_2$, $|\tilde{\mathcal{M}}|^2$ s have been defined below Eq.(1) summing over all initial and final degrees of freedom. For SM pair annihilation, the energy transfer per collision is $E_{\text{trans.}} = E_1 + E_2$. It can be useful to write an analytical approximation for the solution $\rho'(T)$ in the early Universe. Indeed for $T \gg m_{Z',\chi}$, it is easy to show that Eq.(25) reduces to

$$\begin{aligned} \frac{d(\rho'/\rho)}{dT} &\simeq -640 \sqrt{\frac{45}{\pi}} \frac{\alpha \delta^2 M_p}{\pi^7 T^2 g_*^{3/2}} \\ \Rightarrow \left(\frac{T'}{1 \text{ GeV}}\right) &\simeq 3000 \sqrt{\delta} \left(\frac{T}{1 \text{ GeV}}\right)^{3/4} \quad (26) \end{aligned}$$

supposing that the dark bath is in kinetic equilibrium ($\rho' \propto (T')^4$) with $\alpha = g^2/4\pi$ (see next section for more details). Even if all our analysis was made using the analytical solutions of the coupled Boltzmann system, we checked that this analytical solution is a quite good approximation to the exact numerical solution of Eq.(25) and will be very useful to understand the physical phenomena hidden by the numerical results.

While presenting a detailed study of the visible-to-dark energy transfer is out of the scope of this work, we just want to point out that there is typically a moment at which the dark sector (i.e. DM plus Z') is sufficiently populated as for creating particles out of itself, e.g. in processes as a t-channelled $\chi\bar{\chi} \rightarrow Z'Z' \rightarrow 2\chi 2\bar{\chi}$. As this happens out of a total available energy ρ' at any given time, the net effect is to increase n_χ and $n_{Z'}$ at the cost of decreasing T' .

To quantify the effect of DM- Z' chemical equilibrium on the number densities of both particles, we solved the coupled set of their respective Boltzmann equations (see appendix A). The relevant Z' production process is the scattering $\bar{\chi}\chi \rightarrow Z'Z'$ (as compared to $\bar{\chi}\chi \rightarrow Z'$), whereas the relevant Z' depletion process is the decay $Z' \rightarrow \bar{\chi}\chi$ (as compared to $Z'Z' \rightarrow \bar{\chi}\chi$), but of course we have considered all the processes when solving the Boltzmann equations. The results are shown in Fig. (3) for $m_{Z'} > 2m_\chi$ and in Fig. (4) for $m_{Z'} < 2m_\chi$.

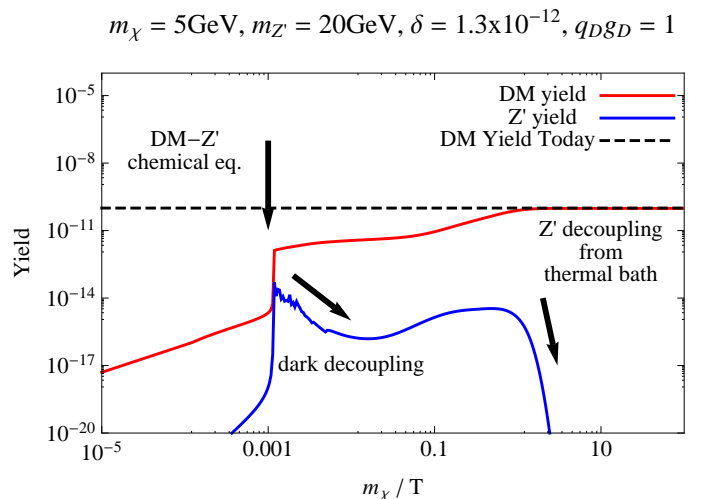


FIG. 3. Evolution of the yield for DM (red) and Z' (blue) as a function of temperature for $m_{Z'} > 2m_\chi$. The set of parameters is given on the figure.

Figure 3 presents several original and interesting features. We can separate the thermal events in 4 phases that we

¹² For a deeper analysis on this, see [48].

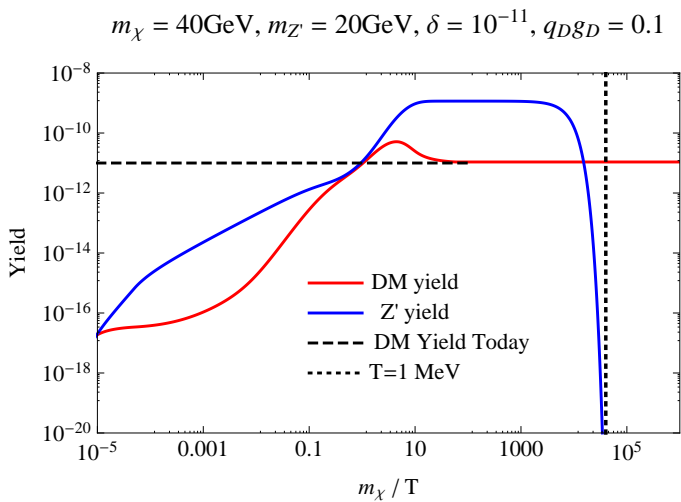


FIG. 4. Same as Fig. (3) with $m_{Z'} < 2m_\chi$. Note here a smaller $q_D g_D$ is adopted to avoid too many dark matter annihilations.

detail below: dark kinetic equilibrium of the dark matter candidate, self exponential production of dark matter through its annihilation, decoupling of the Z' from the dark bath and then decoupling of χ and Z' from the thermal standard bath.

Indeed, we can notice a first kind of plateau for the dark matter yield Y_χ at $T \gg 10^3$ GeV. This corresponds to the time when the dark matter concentration is sufficient to enter equilibrium with itself through the exchange of a virtual Z' (s or t channel). Indeed, the condition $n_\chi \langle \sigma v \rangle > H(T)$ can be expressed as

$$\begin{aligned} \{10^{-5} M_p g_*^s \delta^2 \alpha T^2\} \times \frac{(q_D g_D)^4}{(4\pi)^2 T^2} &> \frac{1.66}{M_p} \sqrt{g_*} T^2 \\ \Rightarrow T &\lesssim 1.6 \times 10^{15} g_*^{1/4} \alpha^{1/2} \delta \text{ GeV} \end{aligned} \quad (27)$$

where we have used an approximate solution of Eq.(1) at high temperatures:

$$Y_\chi \simeq \alpha \delta^2 \frac{10^{14} \text{ GeV}}{T} \quad (28)$$

with $\alpha = \frac{g^2}{4\pi}$. The result is then in accordance with what we observed numerically.

We then observe in a second phase, around $m_\chi/T = 10^{-3}$, a simultaneous and sharp rise in the number density of DM and Z' . This is because the dark sector enters in a phase of chemical equilibrium with itself, causing the population of both species to increase. Moreover, in the case $m_{Z'} > 2m_\chi$, we observe that the width of the Z' $\Gamma_{Z'}$ is much larger than the production rate through the

t channel $\chi\chi \rightarrow Z'Z'$:

$$\begin{aligned} \Gamma_{Z'} &\simeq \frac{(q_D g_D)^2}{16\pi} m_{Z'} \simeq 0.4 \text{ GeV}, \quad (29) \\ n \langle \sigma v \rangle_{\chi\chi \rightarrow Z'Z'} &\simeq 10^{12} g_*^s \delta^2 \alpha (q_D g_D)^4 \\ &\simeq 10^{-12} \sqrt{\frac{T}{1\text{GeV}}} \text{ GeV}. \end{aligned}$$

In other words, as soon as a Z' is produced, it automatically decays into two DM particles before having the time to thermalise or annihilate again. We then observe an exponential production of DM. Of course, each product of the Z' decay possesses half of the initial energy of the annihilating DM, this energy also decreasing exponentially. As a consequence, the temperature of the dark sector, T' , typically drops below $m_{Z'}$ at a certain temperature T such that the dark sector does not have enough energy for maintaining an efficient Z' production¹³. This is illustrated as “dark decoupling” in Fig. (3), where the excess of Z' population decays mostly to DM particles. We can understand this phenomenon by looking more in details at the solution of the transfer of energy (26). Taking $T' \simeq m_{Z'}$ in Eq.(26), we can check that the decoupling of the Z' from the dark bath happens around a temperature $T \simeq 2$ TeV when the DM does not possess sufficiently energy to produce a Z' pair. This result is in accordance with the value observed in Fig. (3) along the arrow labelled *dark decoupling*.

However, the thermal (standard) bath is still able to slowly produce Z' after its decoupling from the dark bath but at a very slow rate (proportional to δ^2) up to the moment at which the temperature T drops below $m_{Z'}$, when the Z' population decays completely as we can also observe in Fig. (3). During this time the DM population increases also slowly due to the annihilation of SM particles through the exchange of a virtual Z' added to the product of the Z' decay until T reaches m_χ .

We also depict in Fig. (4) the evolution of the Z' and DM yields in the case $m_{Z'} < 2m_\chi$. We observe similar features, except that the Z' does not decouple from the dark bath and is not responsible anymore for the exponential production of DM. The DM decouples first from the plasma, and then the Z' continues to be produced at a slow rate, being also largely populated by the t -channel annihilation of the dark matter. However, it never reaches the thermal equilibrium with the thermal bath as it decays to SM particles (at a very low rate proportional to δ^2) at a temperature of about 1 MeV, not affecting the primordial nucleosynthesis (see below for details).

¹³ Strictly speaking one should not use the word *temperature* T' during this very short time but more express ourselves in terms of energy.

3. Cosmological constraints

The PLANCK collaboration [1] recently released its results and confirmed the WMAP [4] non-baryonic content of the Universe. It is then important to study in the $(m_\chi, m_{Z'}, \delta)$ parameter space the region which is still allowed by the cosmological WMAP/PLANCK constraint. As we discussed in the previous section, a small kinetic mixing can be sufficient to generate sufficient relic abundance. We show in Fig. (5) the plane $(\delta, m_{Z'})$ compatible with WMAP/PLANCK data ($\Omega h^2 \simeq 0.12$) for different dark matter masses. Depending on the relative value between m_χ and $m_{Z'}$, we can distinguish four regimes clearly visible in Fig. (5):

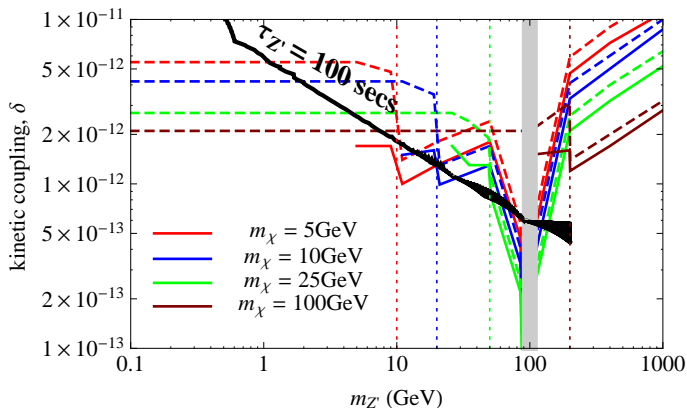


FIG. 5. Kinetic-mixing coupling δ as a function of $m_{Z'}$ for different values of m_χ : 5, 10, 25 and 100 GeV for red, blue, green and brown curves, respectively. These lines are in agreement with WMAP: $\Omega_\chi h^2 \sim 0.12$. We have fixed $q_{DGD} = 1$, as before. Solid lines are obtained taking into account the “dark thermalisation” effect (see text for details) whereas dashed lines are obtained without such an effect. The solid black line shows BBN constraints (see text details), which apply, for each DM mass (shown with dotted lines), to the region $m_{Z'} < 2m_\chi$.

(a) $m_{Z'} < 2m_\chi$. In this regime, the dark matter is mainly produced from the plasma through s -channel exchange of the Z' and then decouples from the thermal bath at $T \simeq m_\chi$. Dark matter then annihilates into two Z' through t -channel process if kinetically allowed (see Fig. 4). For light Z' , the amplitude of dark matter production¹⁴ ($|\mathcal{M}|^2 \propto \delta^2 m_\chi^2 / s \sim \delta^2 m_\chi^2 / T^2$ from Eq.15) and the annihilating rate ($\chi\chi \rightarrow Z'Z'$) after the decoupling time are both independent of $m_{Z'}$. As a consequence, the relic abundance is also independent of $m_{Z'}$ (but strongly dependent of δ) as one can observe in the left region of Fig.(5).

¹⁴ In this region the Z' -SM couplings (see Appendix A) are roughly proportional to δ , since $\sin \phi \ll \delta$ for the values of δ and $m_{Z'}$ in consideration.

(b) $2m_\chi < m_{Z'} < M_{Z'}$. We notice a sharp decrease in the values of δ occurring around $m_{Z'} = 2m_\chi$. Indeed, for $m_{Z'} > 2m_\chi$ there exists a temperature in the plasma for which the resonant production of on-shell Z' is abundant ($T \simeq m_{Z'}/2$). The Z' being unstable, it immediately decays into 2 dark matter particles increasing its abundance. The rate of the dark matter production from the standard model bath around the pole $T \simeq m_{Z'}/2$ is proportional to $\delta^2 m_\chi^2 T^2 / m_{Z'}^2 \Gamma_{Z'}^2$ (Eq.15). This rate is higher than in the region $m_{Z'} < 2m_\chi$ where $|\mathcal{M}|^2 \propto \delta^2 m_\chi^2 / T^2$: δ should then be smaller in order to still respect PLANCK/WMAP constraint.

(c) $m_{Z'} \approx M_{Z'}$. This is the region of maximal mixing: $\phi \approx \pi/4$. The total amplitude of annihilation in Eq.(13) is maximised, driving δ toward very small values in order to respect PLANCK/WMAP constraint. However, this region is excluded by electroweak measurements because of large excess in the ρ parameter (see [43] for a complete analysis in this regime).

(d) $2m_\chi < M_{Z'} < m_{Z'}$. For even larger values of $m_{Z'}$ the amplitude has a smooth tendency of decreasing with $m_{Z'}$ from its dependence on the width. The majority of the dark matter population is indeed created when the temperature of the universe, playing the role of a statistical accelerator with time dependent centre of mass energy, reaches $T \simeq m_{Z'}/2$ (or $m_{Z'}/2$). The production cross section through s -channel exchange of Z' is then proportional to $\delta^2 / m_{Z'}^2 \Gamma_{Z'}^2 \propto \delta^2 / m_{Z'}^4$. Keeping constant final relic abundance implies $\delta^2 / m_{Z'}^4 = \text{constant}$, which is observed in the right region of Fig.(5).

For the sake of completeness, we also show in Fig. (5) the effect of allowing the Z' and dark matter to enter in a phase of chemical equilibrium (solid lines), see Fig. (3) and compare it to the more naive case where no dark-thermalisation is taken into account (dashed lines). We observe that depending on the DM and Z' masses, the correction caused by the dark-thermalisation for $q_{DGD} = 1$ is at most a factor 2.

Meanwhile, a general look at Fig. (5) tells us that the order of magnitude of δ to respect relic abundance data is generally in the range 10^{-12} – 10^{-11} , which is in absolute value of the same order that typical FIMP couplings obtained in the literature for different frameworks [8, 10–13] but with a much richer phenomenology due to the instability of the mediator and the existence of dark thermalisation. It is interesting to note that such tiny kinetic mixing, exponentially suppressed, is predicted by recent work on higher dimensional compactification and string phenomenology to lie within the range $10^{-12} \lesssim \delta \lesssim 10^{-10}$ [37].

Finally, due to the feeble coupling δ , it is important to check constraints coming from Big Bang Nucleosynthesis (BBN) in the specific case $m_{Z'} < 2m_\chi$. Indeed, if Z'

is lighter than the dark matter, the Z' will slowly decay to the particles of the thermal bath, potentially affecting the abundance of light elements. For the ranges of Z' masses we consider here, a naive bound from BBN can be obtained by simply requiring the Z' lifetime to be shorter than $\mathcal{O}(100)$ seconds. This is translated into a lower bound on the kinetic coupling δ , represented by the black solid line in Fig. (5), where the bound applies, for every m_χ (see dotted lines), to the region $m_{Z'} < 2m_\chi$. We see how the BBN bounds strongly constrain the region of lightest Z' , $m_{Z'} \lesssim 1$ GeV for the DM masses considered here. A more detailed study of nucleosynthesis processes in this framework can be interesting but is far beyond the scope of this paper

4. Other constraints

In [43] several low-energy processes have been used in order to constrain the parameter space of the model we analysed. We refer the reader to that work in order to see the study in more details. In this section, we just want to extract one of the strongest bounds, which comes from Electroweak Precision Tests (EWPT). Indeed, since the model modifies the coupling of the Z to all fermions, the decay rate to leptons, for example, is in principle modified. It turns out that a model is compatible with EWPT under the condition

$$\left(\frac{\delta}{0.1}\right)^2 \left(\frac{250\text{GeV}}{m_{Z'}}\right)^2 \lesssim 1. \quad (30)$$

For a very light Z' of $m_{Z'} \sim 1$ GeV, the EWPT constraints require $\delta \lesssim 10^{-4}$, which is well above the WMAP constraints shown in Fig. (5). Also, since the model modifies the Z mass, constraints coming from the deviation of the SM prediction for the parameter $\rho \equiv M_W^2/M_Z^2 c_W^2$ are also expected to appear; however, they turn out to be weaker or similar to those of EWPT.

Direct Detection experiments, led by XENON [50], are able to put much more stronger bounds on the model. The dark matter candidate can scatter off a nucleus through a t -channel exchange of Z or Z' bosons (see e.g. [43][49]). It turns out that for the dark matter and Z' masses considered, the XENON1T analysis is expected to push δ to values $\delta \lesssim 10^{-4}$, to say the strongest. Again here those bounds are not competitive with those shown in Fig. (5).

As an example of constraints coming from indirect detection, we can use synchrotron data. The dark matter particles in the region of the Galactic Centre can annihilate to produce electrons and positrons, which will emit synchrotron radiation as they propagate through the magnetic fields of the galaxy. In [28] the authors constrain the kinetic mixing in the framework of freeze-out. The synchrotron data is able to put bounds on the parameter space of the model, provided that m_χ and $m_{Z'}$ are light enough (less than $\mathcal{O}(100)$ GeV), and for values of

δ compatible with a thermal relic which are much larger than those required to fit a WMAP with a froze-in dark matter. So given the small δ values considered here, the synchrotron bounds are unconstraining.

V. CONCLUSIONS

In this work we have studied the genesis of dark matter by a Z' portal for a spectrum of Z' mass from above the reheating temperature down to a few GeV. Specifically, we have distinguished two regimes: 1) a very massive portal whose mass is above the reheating temperature T_{RH} , illustrated by effective, vector-like interactions between the SM fermions and the DM, and 2) a weak-like portal, illustrated by a kinetic-mixing model with an extra $U(1)$ boson, Z' , which couples feebly to the SM but with unsuppressed couplings to the dark matter, similar to a secluded dark sector.

In the case of very massive portal we solved the system of Boltzmann equations and obtained the expected dependance of the dark matter production with the reheating temperature. By requiring consistency with the WMAP/PLANCK's measurements of the non-baryonic relic abundance, the scale of the effective interaction Λ should be approximatively $\Lambda \simeq 10^{12}$ GeV, for $T_{RH} \approx 10^9$ GeV.

For lighter Z' that couples to the standard model through its kinetic mixing with the standard model $U(1)$ gauge field, we considered Z' masses in the 1 GeV–1 TeV range. The values of the kinetic mixing δ compatible with the relic abundance we obtained are $10^{-12} \lesssim \delta \lesssim 10^{-11}$ depending on the value of the Z' mass. For such values, the constraints coming from other experimental fields like direct or indirect detection and LHC production, become meaningless. However the bounds coming from the Big Bang nucleosynthesis can be quite important. For the study of the dark matter number density evolution, we looked at the effect of chemical equilibrium between dark matter and Z' on the final dark matter population, which turns out for the parameter space we considered to give a correction of at most a factor of 2.

ACKNOWLEDGEMENTS

The authors would like to thank E. Dudas, A. Falkowski, K. Olive, M. Goodsell, T. Hambye, M. Tytgat, E. Fernandez-Martinez and M. Blennow for very useful discussions. This work was supported by the French ANR TAPDMS **ANR-09-JCJC-0146** and the Spanish MICINN's Consolider-Ingenio 2010 Programme under grant Multi- Dark **CSD2009-00064**. X.C. acknowledges the support of the FNRS-FRS, the IISN, the Belgian Science Policy (IAP VI-11). Y.M. and J.Q. acknowledge partial support from the European Union FP7 ITN INVISIBLES (Marie Curie Actions, PITN-GA-2011- 289442), the ERC advanced grant Higgs@LHC

and thanks the Galileo Galilei Institute for Theoretical Physics for the hospitality and the INFN for partial support during the completion of this work. B.Z. acknowledges the support of MICINN, Spain, under the contract FPA2010-17747, as well as the hospitality of LPT, Orsay during the completion of this project.

Appendix A: Boltzmann equations

The relevant processes happening between the dark sector and SM¹⁵, and with itself, are:

- a : $SM\overline{SM} \rightarrow Z'$, and \bar{a} : $SM\overline{SM} \leftarrow Z'$
- b : $\chi\bar{\chi} \rightarrow Z'$, and \bar{b} : $\chi\bar{\chi} \leftarrow Z'$
- c : $Z'Z' \rightarrow \chi\bar{\chi}$, and \bar{c} : $Z'Z' \leftarrow \chi\bar{\chi}$
- d : $\chi\bar{\chi} \rightarrow SM\overline{SM}$, and
 \bar{d} : $\chi\bar{\chi} \leftarrow SM\overline{SM}$.

The Boltzmann equations for the Z' and DM comoving number densities are:

$$\frac{dY_{Z'}}{dT} = \frac{1}{HT} [\Gamma_{\bar{a}}(Y_{Z'}^{eq} - Y_{Z'}) - \Gamma_{\bar{b}}Y_{Z'} + \langle\sigma v\rangle_b Y_\chi^2 \mathbf{s} - \langle\sigma v\rangle_c Y_{Z'}^2 \mathbf{s} + 2\langle\sigma v\rangle_{\bar{c}} Y_\chi^2 \mathbf{s}] \quad (\text{A1})$$

$$\frac{dY_\chi}{dT} = \frac{1}{HT} [\langle\sigma v\rangle_d ((Y_\chi^{eq})^2 - Y_\chi^2) \mathbf{s} - \langle\sigma v\rangle_b Y_\chi^2 \mathbf{s} + \Gamma_{\bar{b}} Y_{Z'} - 2\langle\sigma v\rangle_{\bar{c}} Y_\chi^2 \mathbf{s} + \langle\sigma v\rangle_c Y_{Z'}^2 \mathbf{s}]. \quad (\text{A2})$$

Here in Eq.(A2), in the very first term, we have made use of the chemical equilibrium condition for a process $A \leftrightarrow B\bar{B}$

$$\langle\sigma v\rangle_{BB \rightarrow A} (Y_B^{eq})^2 \mathbf{s} = \Gamma_{A \rightarrow BB} Y_A^{eq}.$$

Besides, in Eq.(A2), the term proportional to $\langle\sigma v\rangle_d$ does not contain the contribution from on-shell Z' , because it is already included in the term going with $\Gamma_{\bar{b}}$. The reason for this, is that the typical time the reaction $SM\overline{SM} \leftrightarrow \chi\bar{\chi}$ takes to happen, is t_{typ} . This period, even if usually very short, is large enough as to consider $t_{\text{typ}} \gtrsim dt$, where dt is the characteristic time interval when solving the Boltzmann equation. In other words, the evolution dictated by the Boltzmann equation is such that there are always physical (on-shell) Z' particles around, which effectively contribute to a Z' decay.

The Boltzmann equation describing the evolution of the energy density transferred from the SM to the dark sector is:

$$\begin{aligned} \frac{d\rho'}{dt} + 3H(\rho' + P') &= \int \prod_{i=1}^4 d^3\bar{p}_i f_1(p_1) f_2(p_2) \\ &\times |\mathcal{M}|^2 (2\pi)^4 \delta^{(4)}(p_{\text{in}} - p_{\text{out}}) \cdot E_{\text{trans.}} \\ &= \frac{1}{2048\pi^6} \int_{4m_\chi^2}^{\infty} ds K_2\left(\frac{\sqrt{s}}{T}\right) T \sqrt{(s - 4m_\chi^2)s} |\tilde{\mathcal{M}}_{12 \rightarrow \chi\bar{\chi}}|^2 \\ &+ \frac{1}{128\pi^4} K_2\left(\frac{m_{Z'}}{T}\right) m_{Z'} T \sqrt{m_{Z'}^2 - 4m_1^2} |\tilde{\mathcal{M}}_{Z' \rightarrow 12}|^2, \quad (\text{A3}) \end{aligned}$$

¹⁵ Here we are not writing the contributions from processes like $SM\gamma \rightarrow SMZ'$ and $SM\overline{SM} \rightarrow \gamma Z'$; but they are taken into account for the numerical analysis.

where 1 and 2 are the initial SM particles and $m_1 = m_2$, $|\tilde{\mathcal{M}}|^2$ s have been defined below Eq.(1) summing over all initial and final degrees of freedom. For SM pair annihilation, the energy transfer per collision $E_{\text{trans.}} = E_1 + E_2$. The pressure P' is:

$$\begin{aligned} P' &= \rho'_{\text{rel}}/3, \\ \rho'_{\text{rel}} &= \rho' - 2n_\chi m_\chi - n_{Z'} m_{Z'}, \end{aligned} \quad (\text{A4})$$

where ρ'_{rel} is the relativistic contribution to the energy density ρ' .

Appendix B: Couplings in kinetic mixing model

In this appendix we show the couplings of fermions (including DM) to the Z and Z' bosons in our model.

The left (L) and right (R) couplings to the Z bo-

son are:

$$\begin{aligned} (c_L)_f &= -\frac{(2g^2 T_{fL} - g'^2 Y_{fL})}{2\sqrt{g'^2 + g^2}} \cos \phi - \frac{g'}{2} Y_{fL} \sin \phi \delta, \\ (c_R)_f &= \frac{1}{2} g' Y_{fR} \left(\frac{g'}{\sqrt{g'^2 + g^2}} \cos \phi - \sin \phi \delta \right), \end{aligned} \quad (\text{B1})$$

for SM fermions f , and

$$c_\chi = q_D g_D \sin \phi \quad (\text{B2})$$

for the DM. Similarly, the couplings to the Z' boson to the SM fermions and DM χ are:

$$\begin{aligned} (c_L)'_f &= -\frac{(2g^2 T_{fL} - g'^2 Y_{fL})}{2\sqrt{g'^2 + g^2}} \sin \phi + \frac{g'}{2} Y_{fL} \cos \phi \delta, \\ (c_R)'_f &= \frac{1}{2} g' Y_{fR} \left(\frac{g'}{\sqrt{g'^2 + g^2}} \sin \phi + \cos \phi \delta \right), \\ c'_\chi &= q_D g_D \cos \phi. \end{aligned} \quad (\text{B3})$$

-
- [1] P. A. R. Ade *et al.* [Planck Collaboration], arXiv:1303.5076 [astro-ph.CO].
- [2] L. Bergstrom, Rept. Prog. Phys. **63** (2000) 793 [hep-ph/0002126].
- [3] G. Bertone, D. Hooper and J. Silk, Phys. Rept. **405** (2005) 279 [hep-ph/0404175].
- [4] G. Hinshaw, D. Larson, E. Komatsu, D. N. Spergel, C. L. Bennett, J. Dunkley, M. R. Nolte and M. Halpern *et al.*, arXiv:1212.5226 [astro-ph.CO].
- [5] H. Dreiner, D. Schmeier and J. Tattersall, arXiv:1303.3348 [hep-ph]; H. Dreiner, M. Huck, M. Kramer, D. Schmeier and J. Tattersall, Phys. Rev. D **87** (2013) 075015 [arXiv:1211.2254 [hep-ph]]; J. Kopp, E. T. Neil, R. Primulando and J. Zupan, Phys. Dark Univ. **2** (2013) 22 [arXiv:1301.1683 [hep-ph]]; M. T. Frandsen, F. Kahlhoefer, A. Preston, S. Sarkar and K. Schmidt-Hoberg, JHEP **1207** (2012) 123 [arXiv:1204.3839 [hep-ph]]; J. Goodman and W. Shepherd, arXiv:1111.2359 [hep-ph]; P. J. Fox, R. Harnik, J. Kopp and Y. Tsai, Phys. Rev. D **85** (2012) 056011 [arXiv:1109.4398 [hep-ph]]; Y. Mambrini and B. Zaldivar, JCAP **1110** (2011) 023 [arXiv:1106.4819 [hep-ph]].
- [6] K. Cheung, P. -Y. Tseng, Y. -L. S. Tsai and T. -C. Yuan, JCAP **1205** (2012) 001 [arXiv:1201.3402 [hep-ph]]; C. R. Das, O. Mena, S. Palomares-Ruiz and S. Pascoli, arXiv:1110.5095 [hep-ph]; C. -L. Shan, arXiv:1103.4049 [hep-ph]; M. Pato, L. Baudis, G. Bertone, R. Ruiz de Austri, L. E. Strigari and R. Trotta, Phys. Rev. D **83** (2011) 083505 [arXiv:1012.3458 [astro-ph.CO]]; G. Bertone, D. G. Cerdeno, M. Fornasa, R. R. de Austri and R. Trotta, Phys. Rev. D **82** (2010) 055008 [arXiv:1005.4280 [hep-ph]]; N. Bernal, A. Goudelis, Y. Mambrini and C. Munoz, JCAP **0901** (2009) 046 [arXiv:0804.1976 [hep-ph]]; O. Mena, S. Palomares-Ruiz and S. Pascoli, Phys. Lett. B **664** (2008) 92 [arXiv:0706.3909 [hep-ph]]; S. Palomares-Ruiz and J. M. Siegal-Gaskins, JCAP **1007** (2010) 023 [arXiv:1003.1142 [astro-ph.CO]]; P. Konar, K. Kong, K. T. Matchev and M. Perelstein, New J. Phys. **11** (2009) 105004 [arXiv:0902.2000 [hep-ph]].
- [7] T. Moroi, H. Murayama and M. Yamaguchi, Phys. Lett. B **303** (1993) 289.
- [8] L. J. Hall, K. Jedamzik, J. March-Russell and S. M. West, JHEP **1003** (2010) 080 [arXiv:0911.1120 [hep-ph]].
- [9] C. E. Yaguna, JCAP **1202** (2012) 006 [arXiv:1111.6831 [hep-ph]].
- [10] X. Chu, T. Hambye and M. H. G. Tytgat, JCAP **1205** (2012) 034 [arXiv:1112.0493 [hep-ph]].
- [11] J. McDonald, Phys. Rev. Lett. **88** (2002) 091304 [hep-ph/0106249].
- [12] C. E. Yaguna, JHEP **1108** (2011) 060 [arXiv:1105.1654 [hep-ph]].
- [13] G. Arcadi and L. Covi, arXiv:1305.6587 [hep-ph].
- [14] Y. Mambrini, K. A. Olive, J. Quevillon and B. Zaldivar, arXiv:1302.4438 [hep-ph].
- [15] Y. Bai, P. J. Fox and R. Harnik, JHEP **1012** (2010) 048 [arXiv:1005.3797 [hep-ph]].
- [16] P. J. Fox, R. Harnik, J. Kopp and Y. Tsai, Phys. Rev. D **84** (2011) 014028 [arXiv:1103.0240 [hep-ph]].
- [17] Y. Mambrini and B. Zaldivar, JCAP **1110** (2011) 023 [arXiv:1106.4819 [hep-ph]].
- [18] J. F. Kamenik and J. Zupan, Phys. Rev. D **84** (2011) 111502 [arXiv:1107.0623 [hep-ph]].
- [19] P. J. Fox, R. Harnik, J. Kopp and Y. Tsai, Phys. Rev. D **85** (2012) 056011 [arXiv:1109.4398 [hep-ph]].
- [20] J. Goodman and W. Shepherd, arXiv:1111.2359 [hep-ph].

- [21] M. T. Frandsen, F. Kahlhoefer, A. Preston, S. Sarkar and K. Schmidt-Hoberg, *JHEP* **1207** (2012) 123 [arXiv:1204.3839 [hep-ph]].
- [22] Y. J. Chae and M. Perelstein, arXiv:1211.4008 [hep-ph].
- [23] X. Gao, Z. Kang and T. Li, *JCAP* **1301** (2013) 021 [arXiv:1107.3529 [hep-ph]].
- [24] A. Rajaraman, T. M. P. Tait and D. Whiteson, *JCAP* **1209** (2012) 003 [arXiv:1205.4723 [hep-ph]].
- [25] I. M. Shoemaker and L. Vecchi, *Phys. Rev. D* **86** (2012) 015023 [arXiv:1112.5457 [hep-ph]].
- [26] J. Kopp, V. Niro, T. Schwetz and J. Zupan, *Phys. Rev. D* **80** (2009) 083502 [arXiv:0907.3159 [hep-ph]].
- [27] J. Kopp, V. Niro, T. Schwetz and J. Zupan, *PoS IDM* **2010** (2011) 118 [arXiv:1011.1398 [hep-ph]].
- [28] Y. Mambrini, M. H. G. Tytgat, G. Zaharijas and B. Zaldivar, *JCAP* **1211** (2012) 038 [arXiv:1206.2352 [hep-ph]].
- [29] P. Gondolo, J. Hisano and K. Kadota, *Phys. Rev. D* **86** (2012) 083523 [arXiv:1205.1914 [hep-ph]].
- [30] P. Langacker, *Rev. Mod. Phys.* **81** (2008) 1199 [arXiv:0801.1345 [hep-ph]].
- [31] R. Foot, X. -G. He, *Phys. Lett.* **B267** (1991) 509-512; R. Foot, H. Lew, R. R. Volkas, *Phys. Lett.* **B272** (1991) 67-70; B. Holdom, *Phys. Lett. B* **166**, 196 (1986); D. Feldman, Z. Liu and P. Nath, *Phys. Rev. D* **75** (2007) 115001 [arXiv:hep-ph/0702123]; S. P. Martin, *Phys. Rev. D* **54** (1996) 2340 [arXiv:hep-ph/9602349]; T. G. Rizzo, *Phys. Rev. D* **59** (1999) 015020 [arXiv:hep-ph/9806397]; F. del Aguila, M. Masip and M. Perez-Victoria, *Nucl. Phys. B* **456** (1995) 531 [arXiv:hep-ph/9507455]; B. A. Dobrescu, *Phys. Rev. Lett.* **94** (2005) 151802 [arXiv:hep-ph/0411004]; T. Cohen, D. J. Phalen, A. Pierce and K. M. Zurek, arXiv:1005.1655 [hep-ph]; Z. Kang, T. Li, T. Liu, C. Tong, J. M. Yang, *JCAP* **1101** (2011) 028. [arXiv:1008.5243 [hep-ph]].
- [32] K. R. Dienes, C. F. Kolda and J. March-Russell, *Nucl. Phys. B* **492** (1997) 104 [hep-ph/9610479].
- [33] D. Feldman, B. Kors and P. Nath, *Phys. Rev. D* **75**, 023503 (2007) [arXiv:hep-ph/0610133].
- [34] M. Cicoli, M. Goodsell, J. Jaeckel and A. Ringwald, arXiv:1103.3705 [hep-th].
- [35] J. Kumar, A. Rajaraman and J. D. Wells, *Phys. Rev. D* **77** (2008) 066011 [arXiv:0707.3488 [hep-ph]].
- [36] M. Goodsell, S. Ramos-Sanchez and A. Ringwald, *JHEP* **1201** (2012) 021 [arXiv:1110.6901 [hep-th]].
- [37] M. Goodsell, J. Jaeckel, J. Redondo and A. Ringwald, *JHEP* **0911** (2009) 027 [arXiv:0909.0515 [hep-ph]]; S. A. Abel, M. D. Goodsell, J. Jaeckel, V. V. Khoze and A. Ringwald, *JHEP* **0807** (2008) 124 [arXiv:0803.1449 [hep-ph]];
- [38] S. Cassel, D. M. Ghilencea and G. G. Ross, *Nucl. Phys. B* **827** (2010) 256 [arXiv:0903.1118 [hep-ph]].
- [39] S. Andreas, M. D. Goodsell and A. Ringwald, *Phys. Rev. D* **87** (2013) 025007 [arXiv:1109.2869 [hep-ph]].
- [40] M. E. Krauss, W. Porod and F. Staub, arXiv:1304.0769 [hep-ph].
- [41] D. Feldman, Z. Liu and P. Nath, *Phys. Rev. D* **75** (2007) 115001 [hep-ph/0702123 [HEP-PH]].
- [42] M. Pospelov, *Phys. Rev. D* **80** (2009) 095002 [arXiv:0811.1030 [hep-ph]].
- [43] Y. Mambrini, *JCAP* **1107** (2011) 009 [arXiv:1104.4799 [hep-ph]]; Y. Mambrini, *JCAP* **1009** (2010) 022 [arXiv:1006.3318 [hep-ph]]; E. J. Chun, J. C. Park and S. Scopel, “Dark matter and a new gauge boson through kinetic mixing,” *JHEP* **1102** (2011) 100 [arXiv:1011.3300 [hep-ph]].
- [44] F. Domingo, O. Lebedev, Y. Mambrini, J. Quevillon and A. Ringwald, arXiv:1305.6815 [hep-ph]; Y. Farzan and A. R. Akbarieh, arXiv:1211.4685 [hep-ph].
- [45] J. Heeck and W. Rodejohann, *Phys. Lett. B* **705** (2011) 369 [arXiv:1109.1508 [hep-ph]].
- [46] E. Dudas, Y. Mambrini, S. Pokorski and A. Romagnoni, *JHEP* **1210** (2012) 123 [arXiv:1205.1520 [hep-ph]]; Y. Mambrini, mechanism,” *JCAP* **0912**, 005 (2009) [arXiv:0907.2918 [hep-ph]]; E. Dudas, Y. Mambrini, S. Pokorski and A. Romagnoni, *JHEP* **0908**, 014 (2009) [arXiv:0904.1745 [hep-ph]]; C. B. Jackson, G. Servant, G. Shaughnessy, T. M. P. Tait and M. Taoso, arXiv:1302.1802 [hep-ph]; C. B. Jackson, G. Servant, G. Shaughnessy, T. M. P. Tait and M. Taoso, *JCAP* **1004**, 004 (2010) [arXiv:0912.0004 [hep-ph]].
- [47] M. Baumgart, C. Cheung, J. T. Ruderman, L. T. Wang and I. Yavin, *JHEP* **0904** (2009) 014 [arXiv:0901.0283 [hep-ph]].
- [48] M. Blennow, E. Fernandez-Martinez and B. Zaldivar, arXiv:1309.7348 [hep-ph].
- [49] G. Arcadi, Y. Mambrini, M. H. G. Tytgat and B. Zaldivar, arXiv:1401.0221 [hep-ph].
- [50] E. Aprile *et al.* [XENON100 Collaboration], *Phys. Rev. Lett.* **107** (2011) 131302 [arXiv:1104.2549 [astro-ph.CO]]; E. Aprile *et al.* [XENON100 Collaboration], *Phys. Rev. Lett.* **105** (2010) 131302 [arXiv:1005.0380 [astro-ph.CO]]; E. Aprile *et al.* [XENON100 Collaboration], *Phys. Rev. Lett.* **109** (2012) 181301 [arXiv:1207.5988 [astro-ph.CO]].